IOPscience iopscience.iop.org

Home Search Collections Journals About Contact us My IOPscience

Electrical conduction mechanisms in natively doped ZnO nanowires

This content has been downloaded from IOPscience. Please scroll down to see the full text.

2009 Nanotechnology 20 015203

(http://iopscience.iop.org/0957-4484/20/1/015203)

View the table of contents for this issue, or go to the journal homepage for more

Download details:

IP Address: 140.113.38.11
This content was downloaded on 25/04/2014 at 11:38

Please note that terms and conditions apply.

Nanotechnology 20 (2009) 015203 (8pp) doi:10.1088/0957-4484/20/1/015203

Electrical conduction mechanisms in natively doped ZnO nanowires

Shao-Pin Chiu[1], Yong-Han Lin[2] and Juhn-Jong Lin[1,2]

[1] Institute of Physics, National Chiao Tung University, Hsinchu 30010, Taiwan
[2] Department of Electrophysics, National Chiao Tung University, Hsinchu 30010, Taiwan

E-mail: jjlin@mail.nctu.edu.tw

Received 10 July 2008, in final form 31 October 2008
Published 5 December 2008
Online at stacks.iop.org/Nano/20/015203

Abstract
Single-crystalline zinc oxide (ZnO) nanowires (NWs) with diameters of 90–200 nm were synthesized by the thermal evaporation method. Four-probe Ti/Au electrodes were made by the standard electron-beam lithography technique, and the intrinsic resistivities, $\rho(T)$, of individual NWs were measured over a wide range of temperature from 300 down to 0.25 K. The temperature behavior of $\rho(T)$ between 300 and 5 K reveals that the intrinsic electrical-transport mechanisms through individual ZnO NWs are due to a combination of the thermal activation conduction and the nearest-neighbor hopping conduction processes. Three distinct activation and hopping contributions with discrete characteristic activation energies are observed. Above about 100 K, the charge transport mechanism is dominated by the thermal activation of electrons from the Fermi level, μ, to the conduction band. Between approximately 20 and 100 K, the charge transport mechanism is due to the activation of electrons from μ to the upper impurity (D^-) band. Between approximately 5 and 20 K, the charge transport mechanism arises from the nearest-neighbor hopping conduction within the lower impurity (D) band. Such unique electrical conduction behaviors can be explained in terms of the intricate material properties (in particular, the presence of moderately high concentrations of n-type defects accompanied with a slight self-compensation) in natively doped ZnO NWs. In one heavily doped NW, a surface-related conduction process manifesting the two-dimensional attributes of quantum-interference transport phenomena is observed. The carrier concentrations in our NWs have been estimated, and they were found to lie close to the critical concentration for the Mott metal–insulator transition.

(Some figures in this article are in colour only in the electronic version)

1. Introduction

Owing to the potential applications in the emerging nanoelectronics and optoelectronics, zinc oxide (ZnO) has recently attracted intense theoretical and experimental attention [1–3]. ZnO is a wide band gap semiconductor with a direct gap of 3.4 eV at room temperature, and is a native n-type material. The n-type characteristics of electronic conduction in nominally undoped ZnO materials are believed to originate from the native defects such as structural imperfections and unintentional impurities. However, the microscopic origins for these native defects (e.g., Zn interstitials, oxygen vacancies, etc), and their corresponding impurity levels, are still under much debate [4–8]. Generally speaking, it is known that the dopant levels are sensitive to the methods of sample preparation and can roughly be categorized into shallow levels and deep levels. The shallow levels lie approximately 30–60 meV below the conduction-band minimum, E_c, while the deep levels lie approximately 100–600 meV below E_c. To fabricate practicable nanoscale devices, such as field-effect transistors (FETs), photodetectors, and gas and chemical sensors, based on ZnO nanostructures [9, 10], it is very important to understand the charge transport mechanisms first, before one may manage to control and tailor the electrical properties to meet the desired specifications. To this end, several electrical-transport measurements on single ZnO nanowires (NWs) have been reported in the literature, but those previous works were all performed with either the two-probe method [11–14] or in an FET configuration [15–18]. In those studies, the contact resistances, which are usually large and

 © 2009 IOP Publishing Ltd Printed in the UK

Table 1. Values of relevant parameters for four natively doped, single-crystalline ZnO NWs and a bulk single crystal. The three Z-L011, Z-f-R and Z-k1 NWs are refereed to as 'semiconducting' NWs, while the Z-d-L NW is referred to as a 'metallic-like' NW. Owing to uncertainties in the NW dimensions, the absolute values of ρ (300 K) are accurate to ≈10%.

Sample	d (nm)	ρ (300 K) (Ω cm)	ρ_1 (Ω cm)	E_1 (meV)	ρ_2 (Ω cm)	E_2 (meV)	ρ_3 (Ω cm)	E_3 (meV)
Bulk	—	59 800	0.028 ± 0.001	367 ± 2	—	—	—	—
Z-L011	200 ± 11	0.078	0.019 ± 0.001	44 ± 1	0.29 ± 0.01	3.7 ± 0.1	1.7 ± 0.2	0.53 ± 0.04
Z-f-R	87 ± 10	0.078	0.031 ± 0.001	28 ± 1	0.59 ± 0.05	4.8 ± 0.3	4.3 ± 0.1	0.94 ± 0.05
Z-k1	103 ± 5	0.15	0.051 ± 0.003	34 ± 1	0.71 ± 0.05	4.0 ± 0.2	9.1 ± 1.7	0.53 ± 0.07
Z-d-L	125 ± 6	0.019	—	—	—	—	—	—

strongly temperature dependent, can greatly complicate the measured resistances $R(T)$ of the NW devices. As a result, the conclusions drawn from such measurements are often doubtful. For instance, it has been suggested that the variable-range hopping (VRH) conduction is the prevailing charge transport process in individual ZnO NWs [12]. (In contrast, in the present work, we shall show that the conduction mechanisms in single-crystalline ZnO NWs are due to a combination of the thermal activation and the nearest-neighbor hopping (NNH) conduction processes.) In fact, the *intrinsic* electrical-transport properties of *individual* ZnO NWs can by no means be resolved by employing the two-probe measurement configuration. The four-probe method over a broad range of temperature must be utilized to unambiguously uncover the intrinsic electrical resistivities, $\rho(T)$, of ZnO NWs.

In this work, we have carried out four-probe measurements over a very wide range of temperature from 300 down to 0.25 K to investigate the temperature behavior of resistivities in single ZnO NWs. Our objective is to provide an in-depth physical explanation for the electrical conduction mechanisms in this scientifically and industrially alluring semiconductor NW system. It might sound surprising to say that, even after a few decades of research efforts [2, 3], together with recent resurgence of much focused attention [10], the electrical-transport properties in all forms (bulks, films and NWs) of ZnO materials still remain fairly mysterious. The results of this work will help us to gain insight into the nontrivial electronic conduction mechanisms in ZnO NWs (as well as in bulks and films). A good understanding of the electrical conduction processes is a first step for the fabrication of feasible ZnO nanoelectronic and optoelectronic devices.

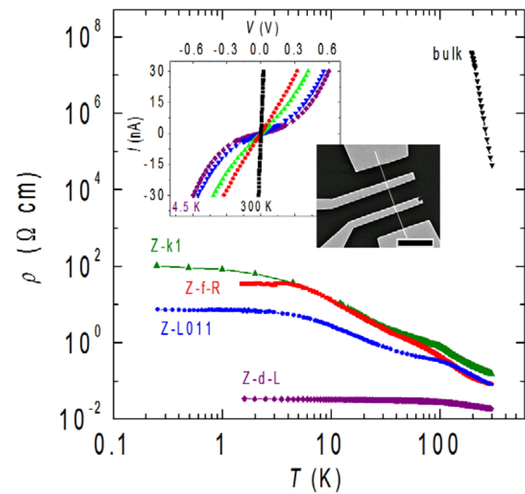

Figure 1. Variation of resistivity with temperature for four ZnO NWs and a bulk ZnO single crystal. The inset shows the current–voltage curves for the Z-k1 NW at 300, 30, 20, 10 and 4.5 K. Also shown is a SEM image for a four-probe NW device fabricated with electron-beam lithography. The scale bar is 5 μm. Notice that the resistivities of the natively doped NWs are several orders of magnitude lower than that of the bulk.

2. Experimental method

ZnO NWs were grown on quartz substrates by the standard thermal evaporation method, as has been described previously [19]. ZnO powders were placed in a quartz tube and were heated to 950 °C. An argon gas with a constant flow rate was input from one end of the tube to carry the evaporated ZnO to several quartz substrates which were placed in the other end of the tube and held at 500 °C. With the use of 100 nm Au nanoparticles as catalysts, the NWs were grown along the [0001] direction (c axis). X-ray diffraction and transmission electron microscopy studies indicated that the NWs were single crystalline, having a wurtzite structure, and possessed a circular cross section [19]. Four single ZnO NWs with diameters in the range 90–200 nm and a few microns long were chosen for the present experiment. The relevant parameters for the NWs studied are listed in table 1.

To fabricate individual NW devices for four-probe electrical measurements, we first made micron-sized Ti/Au (10/60 nm) pads on a Si substrate which was capped with a 400 nm thick SiO_2 layer. ZnO NWs were then dispersed on the SiO_2-capped Si substrate. Individual ZnO NWs were identified and electrically connected to the micron-sized pads by utilizing standard electron-beam lithography and the lift-off technique. The electrodes were made of thermally evaporated Ti/Au (20/120 nm) films, as described previously [20]. A scanning electron microscopy (SEM) image of a representative four-probe NW device is shown in the inset to figure 1.

To improve the signal-to-noise ratio in electrical measurements, we had performed post-annealing at 300 °C for 10–20 min in a high vacuum, which greatly reduced the contact resistances to a few kΩ at room temperature. Four-probe DC measurements had been carried out, utilizing a Keithley K-220 or K-6430 as a current source and a high-impedance (TΩ) Keithley K-617 or K-6430 as a voltmeter. The NW devices were placed on a sample holder which was situated inside a dark vacuum can. The vacuum can was mounted on a standard ^{4}He cryostat or an Oxford Heliox ^{3}He fridge. It should be noted

that the resistances reported in this work were all measured by scanning the current–voltage (I–V) curves at various fixed temperatures between 300 and 0.25 K. The resistance at a given temperature was then determined from the regime around the zero bias voltage, where the I–V curve was essentially *linear*. Notice that, since we had employed the four-probe configuration, the measured resistances (resistivities) were thus the intrinsic resistances (resistivities) of the individual NWs. For comparison, we had also measured the $\rho(T)$ of a bulk ZnO single crystal near room temperature.

3. Results and discussion

Figure 1 shows our measured resistivities $\rho(T)$ as a function of temperature for four individual NWs and a bulk ZnO single crystal. The inset shows the I–V curves for the Z-k1 NW at five different measurement temperatures. This figure clearly demonstrates that the resistivities increase monotonically with decreasing temperature, as would be expected for semiconductors. For comparison, we notice that the room-temperature resistivity of the bulk is 5–6 orders of magnitude higher than those of the NWs. The considerably low resistivity values of our as-grown NWs are strongly suggestive of the presence of high concentrations of native defects (dopants) in the NWs. In particular, the unintentional doping concentration is so high that the Z-d-L NW reveals metallic impurity conduction behavior [21], namely, the resistivity becomes almost temperature independent below about 70 K. For the convenience of discussion, we shall denote this Z-d-L NW as being *heavily* doped and 'metallic-like'. For the other three NWs (Z-k1, Z-f-R and Z-L011), we shall denote them as being *moderately* doped and semiconducting. We shall see below that the three semiconducting NWs lie just below, while the metallic-like NW lies just above, the Mott metal–insulator transition.

3.1. Semiconducting ZnO nanowires

In this work, we measured the resistivities over a broad range of temperature from 300 down to 0.25 K. Studies of the overall temperature behavior of resistivities will help to shed light on the microscopic charge transport mechanisms in this prominent material. Figure 2(a) shows the variation of the resistivity with reciprocal temperature for the three semiconducting NWs between 300 and 4 K. The symbols are the experimental data and the solid curves are least-squares fits to the following equation:

$$\rho^{-1}(T) = \rho_1^{-1}\,e^{-E_1/k_B T} + \rho_2^{-1}\,e^{-E_2/k_B T} + \rho_3^{-1}\,e^{-E_3/k_B T}, \quad (1)$$

where ρ_i ($i = 1, 2, 3$) are temperature-independent resistivity parameters, and E_i are thermal activation energies describing the electronic conduction in the high (E_1), intermediate (E_2), and low (E_3) temperature regimes. Notice that $E_1 > E_2 > E_3$ and $\rho_1 \ll \rho_2 \ll \rho_3$, as is evidenced in figure 2(a). Our experimental values of E_is and ρ_is are listed in table 1. As for illustrations, the three straight dashed lines indicate the three contributions given by equation (1) for each NW. Below a few degrees kelvin, the resistivities progressively cross over

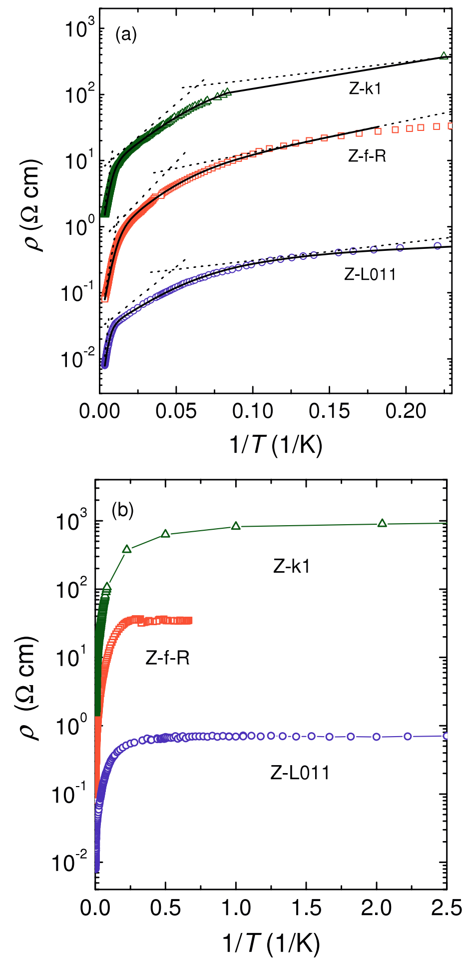

Figure 2. (a) Variation of resistivity with reciprocal temperature for three semiconducting ZnO NWs between 300 and 4 K. The solid curves are least-squares fits to equation (1). The straight dashed lines indicate the three contributions given by equation (1) for each NW. (b) Variation of resistivity with reciprocal temperature for the same three semiconducting ZnO NWs between 300 and 0.4 K. Notice that the resistivity essentially approaches a constant below 2–4 K in each NW. The solid curves are guides to the eye. In both (a) and (b), for clarity, the resistivity of the Z-k1 NW has been vertically shifted up by multiplying a factor of 10, while the resistivity of the Z-L011 NW has been vertically shifted down by multiplying a factor of 0.1.

to a very weakly temperature-dependent regime. Figure 2(b) shows a plot of the variations of resistivity with reciprocal temperature for the same three NWs from 300 K down to 0.4 K. A metallic-type regime with an essentially constant resistivity below 2–4 K is clearly found in every NW. We first discuss the temperature regime between 300 and 5 K where equation (1) is applicable.

The physical origin for the seemingly nontrivial temperature behavior described by equation (1), which contains three additive terms, can be understood in terms of the intricate material properties of nominally undoped ZnO materials. This is particularly true for ZnO NWs, where unintentional doping is often more pronounced than that in films and bulks [22]. This material property resulting complexity can partly explain why the conduction mechanisms in ZnO have remained largely unclear even after a few decades of extensive research efforts.

Figure 3 depicts a schematic electronic density of states (DOS) diagram that could lead to the charge transport processes described by equation (1) [23, 24]. We first explain how the material properties of ZnO NWs would give rise to the formation of a band structure like this. Then, we interpret our experimental results in figure 2(a) in terms of such a specific band structure. We also mention in passing that, due to the large energy gap of 3.4 eV in ZnO, the thermal excitations of carriers from the valence band to the conduction band will not occur at our measurement temperatures ($\lesssim$300 K). Therefore, the valence band can be totally ignored in the following discussion.

It is well accepted that as-grown ZnO NWs are often moderately (and, sometimes, highly) doped with native n-type defects [15–18]. According to the current understanding, the major impurity levels of isolated shallow defects in this material lie approximately 30–60 meV below E_c. However, due to the moderate-to-heavy unintentional doping, the random Coulomb fields arising from the compensating acceptors and ionized donors will cause the donor levels to disperse into an impurity band [25]. Moreover, the impurity band could further split into two bands, i.e., the lower D band and the upper D$^-$ band [23, 24, 26]. The former is formed with singly charged donors while the latter is formed with neutral donors. In general, the D$^-$ band is comparatively wider than the D band, because the singly filled neutral donor orbital is relatively larger than the singly charged donor orbital [27]. Furthermore, such large fluctuations in the Coulomb potential might also cause the tails of the two impurity bands as well as the bottom tail of the conduction band to smear into the forbidden gaps. The smearing could be so significant that the edge states from neighboring bands overlap, forming localized regimes with finite DOS. (The localized regimes are hatched with dotted lines in figure 3.) For moderately doped n-type ZnO NWs (which are pertinent to our three semiconducting NWs), the Fermi level, μ, lies inside the lower D band. The electronic levels below μ are occupied (denoted by the shaded regime in figure 3), while the levels above μ are unoccupied, at zero temperature. The presence of a small number of unoccupied levels above μ is a direct consequence of a *slight self-compensation* which *always* takes place in nominally undoped ZnO NWs [28, 29]. In the case of a weak compensation, μ lies near the top edge of the D band.

The electrical conduction processes described by equation (1) can now be explained. Near room temperature, the electrons are thermally excited from the Fermi level μ (i.e., the donor ground state) to the conduction band where a huge amount of unoccupied, extended states with high mobilities are available. (Therefore, equation (1) describes the electrical conduction well below the 'exhaustion region'.) This thermal activation process is responsible for the measured E_1-conduction channel. Our measured activation energies of $E_1 \approx$ 28–44 meV in the three semiconducting NWs are in good accord with the current knowledge of the ionization energy for the major shallow donors in the ZnO materials [9, 10, 28]. The exact thermal ionization energies in different NWs will differ somewhat due to variations in the donor and compensator concentrations. It has been argued that these shallow donors originate from Zn interstitials, O vacancies, or incidental hydrogen doping [4, 5, 7, 8, 30]. Nevertheless, a consensus has not been reached to date.

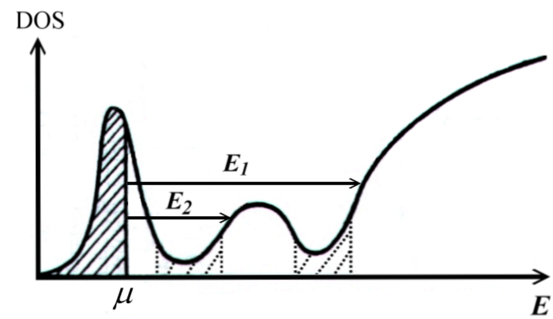

Figure 3. Schematic electronic density of states (DOS) diagram depicting the conduction band (E_1-conduction) and the upper D$^-$ band (E_2-conduction) processes. The impurity band splits into two bands: the lower D band and the upper D^{-1} band. If disorder is strong enough, the band tails will smear and overlap, leading to localized regimes with finite DOS (as hatched with dotted lines). In the case of a weak compensation, the Fermi level μ lies near the top edge of the lower D band. The presence of a small number of unoccupied donor levels which lie just above μ is not explicitly indicated. (See, for example, references [24] and [26].)

As the temperature decreases to approximately 100 K, the thermal energy $k_B T$ (k_B is the Boltzmann constant) is no longer favorable to excite the electrons from μ to the conduction band. Instead, the electrons may now be excited to the middle of the upper D$^-$ band where unoccupied states are available and the carrier mobilities are relatively large, as compared with the *hopping* mobilities associated with the levels around μ. (Due to a much larger donor orbital, the wavefunction overlapping in the D$^-$ band far exceeds that in the D band, giving rise to a much higher mobility.) As a result, the E_2-conduction process is experimentally realized in our semiconducting ZnO NWs at intermediate temperatures between approximately 20 and 100 K. It is important to recall that the predominant shallow donor ionization energy is sufficiently large ($\gtrsim$30 meV) in the ZnO materials. Therefore, the E_1-conduction process cannot persist down to a few tens of degrees kelvin. Otherwise, the E_2-conduction regime would be squeezed and might hardly be seen in the experiment. Our measured values of E_2 are $\approx$4–5 meV. These extracted values are fairly reasonable, as E_2 is theoretically one half the energy gap from the Fermi level μ to the bottom (or, the lower mobility edge) of the D$^-$ band [23]. To the best of our knowledge, the E_2-conduction mechanism has never been found in ZnO materials and any other semiconductor NWs thus far.

As the temperature further reduces to below 20 K, the thermal energy $k_B T$ eventually becomes too small to excite the electrons from μ to the D$^-$ band. In this case, the NNH conduction of electrons across μ becomes the dominant charge transport process. The electrons are excited from the occupied levels (neutral centers) lying slightly below μ to nearby, or the nearest-neighbor, unoccupied levels (ionized centers) lying slightly above μ. Such a phonon-assisted conduction mechanism only involves those levels falling within a narrow energy range ($\sim k_B T$) around μ. This is the E_3-, or the NNH,

conduction process. As a consequence, one immediately sees that the activation energy E_3 must assume small values ($E_3 < E_2 < E_1$). Our extracted values of E_3 are $\approx 0.7 \pm 0.2$ meV (see table 1). It should be stressed that NNH conduction can occur at low temperatures in this particular material, because the unintentionally doped ZnO NWs are always slightly self-compensated [28, 29], as discussed.

Again, the occurrence of the E_2-conduction process is a subtle issue which is closely associated with the unique and complex material properties of unintentional doped ZnO NWs. On one hand, it requires a sufficiently high concentration of dopants so that the formation of the upper D^- band, splitting from the lower D band, is substantiated. On the other hand, the degree of self-compensation in the NWs should be low such that $N_D \gg N_A$, where N_D is the donor concentration and N_A is the acceptor concentration. Otherwise, in the presence of many unoccupied donor levels above μ due to a high compensation, the NNH conduction process may persist up to sufficiently high temperatures. Thus, the inherently bounded temperature regime that could be pertinent to the E_2-conduction mechanism will be squeezed. Previously, the E_2-conduction process has only been found in very carefully doped as well as compensated semiconductors Ge [31–33], CdTe [34], GaAs [35], $GaInP_2$ [36, 37], and Ge:Sb [38].

For the three semiconducting ZnO NWs that we have studied, the values of E_i (i = 1, 2 or 3) are similar (see table 1). Moreover, both the crossover temperature (∼100 K) from the E_1-conduction to the E_2-conduction channels and that (∼20 K) from the E_2-conduction to the E_3-conduction channels are similar. These results provide a consistency check of our experimental method and our interpretation based on the specific band structure given in figure 3. Since these three NWs were grown simultaneously and have similar room-temperature resistivities (and hence similar donor concentrations, see below), they should possess resemblant band structures, and thus their overall temperature behaviors of the resistivity should be alike. It should be emphasized that our measured $\rho(T)$ shown in figure 2(a) cannot be fitted with only two conduction channels, for example, by ignoring the second term and setting $\rho_2 = \infty$ in equation (1).

Figure 2(b) indicates that, in every semiconducting NW, the resistivity eventually approaches a constant below about 2–4 K. A temperature-independent resistivity implies a metallic-like behavior. This result suggests that these NWs should contain high levels of native defects and fall close to the metal–insulator transition. Owing to the presence of such a metallic-like conduction channel (which is not included in equation (1)), the NNH conduction term discussed above can only be observed down to around 5 K. Besides, a crossover from the NNH conduction to the VRH conduction processes at very low temperatures is not to be seen in these NWs [24].

Now we briefly comment on the previous two-probe measurements of $\rho(T)$ on individual ZnO NW devices [11–13]. In the recent experiment of Ma *et al* [12], it has been concluded that the electrical-transport mechanism is due to VRH conduction, i.e., the measured resistances are described by $R = R_0 \exp(T_0/T)^{1/2}$, where R_0 is a resistance parameter, and T_0 is a characteristic temperature. The exponent 1/2 was explained as arising from the VRH conduction in the presence of Coulomb correlation effects [24]. This result is clearly in sharp contrast to our observations discussed above. In fact, we speculate that the VRH result likely reflects the measured magnitude and temperature behavior of the contact resistance(s) formed at the interface(s) between the ZnO NW and the metal electrode(s). To testify this assertion, we have recently demonstrated [19] that, in two-probe individual ZnO NW devices, the measured resistance can manifest either a $R \propto \exp(T_0/T)^{1/2}$ behavior characteristic of the VRH conduction, or a $R \propto \exp(E_a/T)$ behavior characteristic of the thermal activation conduction, where E_a is an activation energy. Which behavior may be observed depends crucially on the measured magnitude of the two-probe device resistance. If the two-probe device resistance is made large (e.g., R (300 K) $\gtrsim$ several hundreds of kΩ, implying that the contact resistance dominates the measured resistance), one would often find the VRH behavior[3]. It is only when the two-probe device resistance is made sufficiently low (e.g., R (300 K) $\lesssim$ several tens of kΩ, implying that the contact resistance is smaller than the NW resistance), may one then find the correct attribute of the thermal activation behavior. In short, one should be very cautious about drawing any conclusion from two-probe measurements.

3.2. ‘Metallic-like’ ZnO nanowire and surface-related conduction

In sharp contrast to the three semiconducting NWs shown in figures 2(a) and (b), the Z-d-L NW reveals ‘metallic-like’ conduction[4]. This is obviously due to a *heavy* doping of native defects in this particular NW. In this case, the resistivity is very low (ρ(300 K) = 0.019 Ω cm) and almost constant (≈0.032 Ω cm) below about 70 K (see figure 1). The most interesting electrical-transport properties of this NW are to be found at low temperatures. A close inspection indicates that the NW resistance increases with the *logarithm* of temperature at liquid-helium temperatures (figure 4). As the temperature reduces from 20 to 1 K, the normalized resistance increases by an amount $\Delta R(T)/R(20\ \mathrm{K}) = [R(1\ \mathrm{K}) - R(20\ \mathrm{K})]/R(20\ \mathrm{K}) \approx 0.04$. This magnitude and the $-\ln T$ behavior suggest that the resistance rise is due to the *two-dimensional* weak-localization and electron–electron interaction effects [41]. (A sheet resistance of $R_\square \approx 1$ kΩ will give rise to the amount of resistance rise found in figure 4.) That is, the electrical transport in this particular NW is *surface-related*, rather than bulk, in nature. This assertion is further supported by the observation of a small and negative magnetoresistance, $-\Delta R(B)/R(0) = -[R(B) - R(0)]/R(0) < 0.01$, in a perpendicular magnetic field and at 4 K.

[3] This assertion has recently been confirmed by an independent study of a 45 nm diameter and 4 μm long two-probe ZnO NW device which had R(300 K) ≈ 3 MΩ. The VRH conduction behavior was observed between 100 and 450 K [39]. The two-probe result in figure 3 of [11], where R(300 K) ≈ 18 MΩ, should also be better described by the VRH conduction, instead of by the thermally activated conduction, as originally proposed by the authors.

[4] Alternatively, one may say that the thermal activation energy from μ to the upper D^{-1} band approaches zero, i.e., $E_2 \to 0$. In this case, E_2 and E_3 become indistinguishable [40].

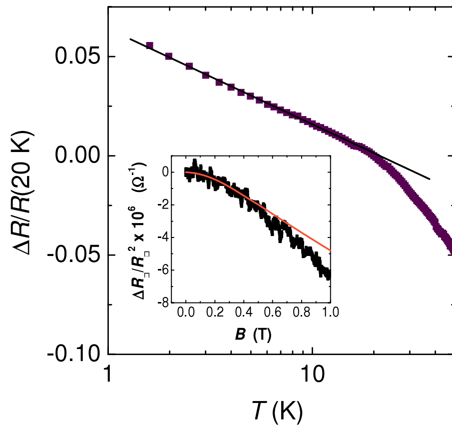

Figure 4. Normalized resistance, $\Delta R(T)/R(20\text{ K}) = [R(T) - R(20\text{ K})]/R(20\text{ K})$, as a function of temperature for the metallic-like Z-d-L NW, where $R(20\text{ K}) = 98.6\text{ k}\Omega$. The straight solid line is a least-squares fit to the two-dimensional weak-localization and electron–electron interaction effects. The inset shows the normalized sheet magnetoresistance, $\Delta R_\square(B)/R_\square^2(0) = [R_\square(B) - R_\square(0)]/R_\square^2(0)$, for the same NW at 4.2 K. The solid curve is a least-squares fit to the two-dimensional weak-localization magnetoresistance theory (see text).

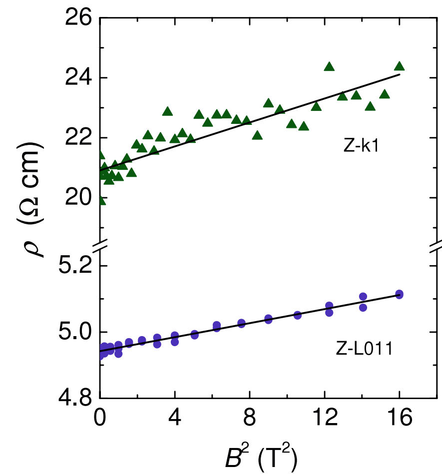

Figure 5. Magnetoresistivity as a function of the square of magnetic field for the Z-k1 NW at 0.255 K (triangles), and the Z-L011 NW at 4.24 K (circles). The straight solid lines are least-squares fits to the data.

The negative magnetoresistance can be ascribed to the suppression of the two-dimensional weak-localization effect in the presence of an externally applied magnetic field [41, 42]. (Notice that in magnetic fields of $\lesssim 1$ T, the electron–electron interaction effects cause a negligible magnetoresistance.)

The inset to figure 4 shows a least-squares fit of the two-dimensional weak-localization magnetoresistance theory [43] (the solid curve) to the measured data (the symbols), with the characteristic electron dephasing field $H_\varphi = \hbar/4eL_\varphi^2$ as the adjusting parameter, where $L_\varphi = \sqrt{D\tau_\varphi}$ is the electron dephasing length, D is the electron diffusion constant, and τ_φ is the electron dephasing time. By taking the spin–orbit scattering time $\tau_{\text{so}} \gg \tau_\varphi$, we obtain $L_\varphi \sim 30$ nm. (The deviation of the theoretical prediction from the experimental data in the magnetic fields $B \gtrsim 0.5$ T is expected, since the weak-localization effect is most relevant in the low-B regime.) The criterion for the two-dimensional weak-localization effect to prevail suggests that the thickness of the surface-related conducting layer, t, should satisfy the inequality $t \ll L_\varphi$. Thus, it is plausible to conclude that t is less than a few nanometers thick. It is worth noting that the diameter d of this particular NW is 125 nm. If the diameter were much thinner (i.e., if $d < L_\varphi$ and $d < L_T = \sqrt{D\hbar/k_B T}$, the electron thermal diffusion length), one might have found one-dimensional, instead of two-dimensional, weak-localization and electron–electron interaction effects [41, 42, 44].

Therefore, in this highly doped metallic-like NW, surface-related conduction vividly manifests itself through the two-dimensional quantum-interference transport phenomena at low temperatures. In contrast, in the three semiconducting NWs discussed above, there is no evidence in our results that could suggest any reduced-dimensional quantum-interference transport behavior. That is, in the present work, we have no experimental support to argue for a predominant surface-related conduction channel in our semiconducting NWs. This observation is very significant. It provides a powerful probe for a definitive detection of an electron accumulation layer, if any exists, in an NW. This work thus suggests that, in as-grown ZnO NWs, dominant surface-related conduction occurs only in heavily doped samples. If this is the case, the role of an electron accumulation layer in ZnO NWs might have often been overemphasized in the literature [13, 45, 46]. The issue requires further investigations.

For comparison, we point out that the measured magnetoresistances are positive in our semiconducting ZnO NWs at liquid-helium temperatures. Figure 5 shows the magnetoresistivity at 0.255 K for the Z-k1 NW (triangles) in perpendicular magnetic fields. Notice that the magnetoresistivity varies approximately with the square of magnetic field and reaches a large magnitude of $[\rho(4\text{ T}) - \rho(0)]/\rho(0) \approx 0.18$. Such magnetoresistance behavior differs significantly from the small and negative magnetoresistance behavior found in the metallic-like NW discussed above. A positive and quadratic magnetic-field-dependent magnetoresistivity has also been found in the semiconducting Z-L011 NW (circles, figure 5) which has a low-temperature resistivity about one order of magnitude smaller than that in the Z-k1 NW. The origin and properties of the positive magnetoresistance in these semiconducting NWs deserve further studies. In short, both the resistivity and magnetoresistivity behaviors found in our semiconducting and metallic-like NWs are markedly distinct. These results provide clues to the idea that the electrical-transport properties found in the semiconducting NWs reflect bulk conduction properties while those found in the metallic-like NW largely reflect surface-related conduction properties.

3.3. Estimate of carrier concentrations and the metal–insulator transition

To understand the microscopic electronic properties in semiconductor NWs, the carrier concentration is one of

the most important physical quantities to be obtained. Unfortunately, due to the small transverse dimensions of a single NW, one cannot readily perform the conventional Hall coefficient measurements to experimentally extract the carrier concentration, n, in a given sample. Fortunately, it has previously been well established that, in ZnO materials at room temperature, the carrier concentration n obeys a close correlation with the resistivity, being independent of the (film or bulk) form as well as the preparation method of the sample [47]. Therefore, we may follow this robust empirical correlation, namely, figure 4 in [47], to estimate the carrier concentrations in our NWs whose diameters are sufficiently large ($d \approx$ 90–200 nm). For our three semiconducting NWs with $\rho(300\ \text{K}) \approx 0.1\ \Omega$ cm, we estimate the carrier concentrations to be $n \sim 6 \times 10^{17}$ cm^{-3}.[5] This value is in agreement with those values found in many nominally undoped ZnO NWs grown by various groups, where electron concentrations of the orders 10^{17}–10^{18} cm^{-3} are often reported [15–18]. Moreover, this value of $\sim 6 \times 10^{17}$ cm^{-3} is reasonably in line with the theoretically predicted Mott critical concentration, n_c, governing the metal–insulator transition in a doped semiconductor. For hydrogen-like donors in n-type ZnO NWs, one obtains the effective Bohr radius $a_B \approx 1.7$ nm by taking the effective mass and the dielectric constant of ZnO into account [1, 10]. From the Mott criterion $(n_c)^{1/3} a_B \gtrsim 0.25$ for the metal–insulator transition [48], a simple calculation gives $n_c \approx 3 \times 10^{18}$ cm^{-3} at 300 K (assuming that at this temperature all the donors are ionized)[6]. Considering that many parameters in the ZnO NWs are not precisely known, we may already safely conclude that our semiconducting NWs fall below, but close to, the Mott metal–insulator transition. Moreover, as a crosscheck, recall that the E_2-conduction process can only happen for a bounded range of dopant concentration not far below n_c. Therefore, our observation of the E_2-conduction mechanism in the semiconducting NWs also provides a strong support for the above estimate of n. On the other hand, for the Z-d-L NW, our room-temperature resistivity of $\rho(300\ \text{K}) \approx 0.019\ \Omega$ cm suggests a carrier concentration of $n \sim 1 \times 10^{19}$ cm^{-3}, according to the above-mentioned empirical correlation in [47]. This n value confirms that this particular NW falls slightly above the metal–insulator transition, and thus is metallic-like.

The acceptor concentrations N_A in our NWs cannot be readily determined at this stage. However, previous studies of unintentionally doped ZnO materials often found that the acceptor concentrations are one to two orders of magnitude lower than the donor concentrations N_D [4, 28, 50]. This result is in consistency with the requirement for the E_2-conduction process to occur in our semiconducting NWs, i.e., these samples must be weakly compensated and satisfy the condition $N_A \ll N_D$.

[5] Accepting this n value, we obtain a mobility of $\sim$100 cm^2 V^{-1} s^{-1} at 300 K. This mobility value is in line with those reported in the literature [47].

[6] For comparison, Hutson [49] estimated a critical donor concentration of $n_c \approx 6 \times 10^{18}$ cm^{-3} in ZnO single crystals. This value is in reasonable agreement with our estimate.

4. Conclusion

We have studied the intrinsic electrical conduction properties of individual, single-crystalline ZnO NWs from 300 down to 0.25 K by employing the four-probe method. The resistance at each temperature was determined from the slope of the linear I–V curve around zero bias voltage. The temperature behaviors of resistivity in both the semiconducting and the metallic-like NWs have been carefully measured and the conduction mechanisms satisfactorily explained. We found the coexistence of thermal activation and nearest-neighbor hopping conduction processes in the semiconducting samples, which can be understood in terms of the intricate material properties of nominally undoped ZnO NWs. In particular, these NWs are unique in the sense that they are natively moderately doped as well as slightly self-compensated. The major shallow donor levels lie below the conduction-band minimum by an amount slightly larger than the thermal energy of the room temperature ($\sim$26 meV). As a consequence, as the temperature progressively reduces from 300 down to 5 K, the charge conduction processes change consecutively from conduction-band conduction to upper D^--band conduction, and then to nearest-neighbor hopping conduction. Since the conduction processes depend subtly on the specific band structure of natively doped ZnO NWs, the observation of the E_2-conduction mechanism is a unique characteristic of this particular semiconductor NW system. A predominant surface-related conduction channel manifesting two-dimensional weak-localization and electron–electron interaction effects is observed in a heavily doped, metallic-like NW. Estimates of the carrier concentrations indicate that our semiconducting NWs lie just below, while our metallic-like NW lies just above, the Mott metal–insulator transition.

Acknowledgments

The authors are grateful to Zhong-Yi Wu, Ji-Jung Kai and Fu-Rong Chen for providing us with the ZnO nanowires used in this study, and to Jia Grace Lu for helpful discussions. This work was supported by the Taiwan National Science Council through Grant Nos NSC 95-2120-M-009-002 and NSC 96-2112-M-009-025, and by the MOE ATU Program.

References

[1] Pearton S J, Norton D P, Ip K, Heo Y W and Steiner T 2003 *Superlatt. Microstruct.* **34** 3

[2] Özgür Ü, Alivov Ya I, Liu C, Teke A, Reshchikov M A, Doğan S, Avrutin V, Cho S J and Morkoç H 2005 *J. Appl. Phys.* **98** 041301

[3] Klingshirn C 2007 *Phys. Status Solidi* b **244** 3027

[4] Look D C, Farlow G C, Reunchan P, Limpijumnong S, Zhang S B and Nordlund K 2005 *Phys. Rev. Lett.* **95** 225502

[5] Van de Walle C G 2000 *Phys. Rev. Lett.* **85** 1012

[6] Hofmann D M, Hofstaetter A, Leiter F, Zhou H, Henecker F, Meyer B K, Orlinskii S B, Schmidt J and Baranov P G 2002 *Phys. Rev. Lett.* **88** 045504

[7] Lany S and Zunger A 2007 *Phys. Rev. Lett.* **98** 045501

[8] Selim F A, Weber M H, Solodovnikov D and Lynn K G 2007 *Phys. Rev. Lett.* **99** 085502
[9] Heo Y W, Norton D P, Tien L C, Kwon Y, Kang B S, Ren F, Pearton S J and LaRoche J R 2004 *Mater. Sci. Eng.* R **47** 1
[10] Fan Z and Lu J G 2005 *J. Nanosci. Nanotechnol.* **5** 1561
[11] Heo Y W, Tien L C, Norton D P, Kang B S, Ren F, Gila B P and Pearton S J 2004 *Appl. Phys. Lett.* **85** 2002
[12] Ma Y J, Zhang Z, Zhou F, Lu L, Jin A and Gu C 2005 *Nanotechnology* **16** 746
[13] Lin X, He X B, Yang T Z, Guo W, Shi D X, Gao H J, Ma D D D, Lee S T, Liu F and Xie X C 2006 *Appl. Phys. Lett.* **89** 043103
[14] Schlenker E, Bakin A, Weimann T, Hinze P, Weber D H, Gölzhäuser A, Wehmann H H and Waag A 2008 *Nanotechnology* **19** 365707
[15] Fan Z, Wang D, Chang P C, Tseng W Y and Lu J G 2004 *Appl. Phys. Lett.* **85** 5923
[16] Goldberger J, Sirbuly D J, Law M and Yang P 2005 *J. Phys. Chem.* B **109** 9
[17] Chang P C, Chien C J, Stichtenoth D, Ronning C and Lu J G 2007 *Appl. Phys. Lett.* **90** 113101
[18] Song S, Hong W K, Kwon S S and Lee T 2008 *Appl. Phys. Lett.* **92** 263109
[19] Lin Y F, Jian W B, Wang C P, Suen Y W, Wu Z Y, Chen F R, Kai J J and Lin J J 2007 *Appl. Phys. Lett.* **90** 223117
[20] Lin Y H, Chiu S P and Lin J J 2008 *Nanotechnology* **19** 365201
[21] Mott N F and Twose W D 1961 *Adv. Phys.* **10** 107
[22] Wu Z Y, Chen I J, Lin Y F, Chiu S P, Chen F R, Kai J J, Lin J J and Jian W B 2008 *New J. Phys.* **10** 033017
[23] Nishimura H 1965 *Phys. Rev.* **138** A815
[24] Shklovskii B I and Efros A L 1984 *Electronic Properties of Doped Semiconductors* (New York: Springer)
[25] Hung C S and Gliessman J R 1954 *Phys. Rev.* **96** 1226
[26] Mott N F and Davis E A 1979 *Electronic Processes in Non-Crystalline Materials* (Oxford: Clarendon)
[27] Norton P 1976 *Phys. Rev. Lett.* **37** 164
[28] Look D C, Coskun C, Claflin B and Farlow G C 2003 *Physica* B **340–342** 32
[29] Daunov M I, Arslanov R K, Gadjialiev M M, Kortunova E V, Khokhlachev P P and Shvansky P P 2006 *Semiconductors* **40** 1255
[30] Seager C H and Myers S M 2003 *J. Appl. Phys.* **94** 2888
[31] Fritzsche H 1955 *Phys. Rev.* **99** 406
[32] Sadasiv G 1962 *Phys. Rev.* **128** 1131
[33] Davis E A and Compton W D 1965 *Phys. Rev.* **140** A2183
[34] Gu J, Kitahara T, Kawakami K and Sakaguchi T 1975 *J. Appl. Phys.* **46** 1184
[35] Sites J R and Nedoluha A K 1981 *Phys. Rev.* B **24** 4309
[36] Driessen F A J M, Bauhuis G J, Olsthoorn S M and Giling L J 1993 *Phys. Rev.* B **48** 7889
[37] Bauhuis G J, Driessen F A J M and Giling L J 1993 *Phys. Rev.* B **48** 17239
[38] Agrinskaya N V, Kozub V I, Polyanskaya T A and Saidov A S 1999 *Semiconductors* **33** 135
[39] Chang P C and Lu J G 2008 *Appl. Phys. Lett.* **92** 212113
[40] Mott N F and Davis E A 1968 *Phil. Mag.* **17** 1269
[41] Lin J J and Giordano N 1987 *Phys. Rev.* B **35** 545
[42] Lin J J and Bird J P 2002 *J. Phys.: Condens. Matter* **14** R501
[43] Hikami S, Larkin A I and Nagaoka Y 1980 *Prog. Theor. Phys.* **63** 707
[44] Chiquito A J, Lanfredi A J C, de Oliveira R F M, Pozzi L P and Leite E R 2007 *Nano Lett.* **7** 1439
[45] Look D C, Claflin B and Smith H E 2008 *Appl. Phys. Lett.* **92** 122108
[46] Schmidt O, Kiesel P, Ehrentraut D, Fukuda T and Johnson N M 2007 *Appl. Phys.* A **88** 71
[47] Ellmer K 2001 *J. Phys. D: Appl. Phys.* **34** 3097
[48] Mott N F 1982 *Proc. R. Soc.* A **382** 1
[49] Hutson A R 1957 *Phys. Rev.* **108** 222
[50] Look D C, Reynolds D C, Sizelove J R, Jones R L, Litton C W, Cantwell G and Harsch W C 1998 *Solid State Commun.* **105** 399